An Ultradense Polymorph of Rutile with Seven-Coordinated Titanium from the Ries Crater

Ahmed El Goresy,[1,3]* Ming Chen,[1,2] Leonid Dubrovinsky,[3] Philippe Gillet,[4] Günther Graup[1]

We report the discovery of an ultradense post-rutile polymorph of titanium dioxide in shocked gneisses of the Ries crater in Germany. The microscopic diagnostic feature is intense blue internal reflections in crossed polarizers in reflected light. X-ray diffraction studies revealed a monoclinic lattice, isostructural with the baddeleyite ZrO_2 polymorph, and the titanium cation is coordinated with seven oxygen anions. The cell parameters are as follows: a = 4.606(2) angstroms, b = 4.986(3) angstroms, c = 4.933(3) angstroms, β (angle between c and a axes) = 99.17(6)°; space group $P2_1/c$; density = 4.72 grams per cubic centimeter, where the numbers in parentheses are standard deviations in the last significant digits. This phase is 11% denser than rutile. The mineral is sensitive to x-ray irradiation and tends to invert to rutile. The presence of baddeleyite-type TiO_2 in the shocked rocks indicates that the peak shock pressure was between 16 and 20 gigapascals, and the post-shock temperature was much lower than 500°C.

The response of TiO_2 to high pressure has been a subject of many recent experimental investigations (*1–11*). Because rutile is isostructural with stishovite (SiO_2), its behavior at high pressures and temperatures has been considered to offer an analogy that would allow the mechanisms and path of post-stishovite phase transitions to be explored under more convenient laboratory conditions. High-pressure experiments on TiO_2 revealed the existence of several high-pressure polymorphs (*3*, *7–9*). However, until recently, the nature and stability fields of some of these polymorphs and the path of the phase transitions have remained controversial (*1*, *3*, *6*, *7*, *12*, *13*). Rutile is the most abundant species in nature among the low-pressure polymorphs and is a minor constituent in igneous and metamorphic rocks (*14*). The response of TiO_2 to static and dynamic high pressure may thus reveal fundamental information about the behavior of this and other related oxides in Earth's mantle during the subduction of crustal limbs in Earth's interior and natural dynamic events. An α-PbO_2–structured polymorph has been recently reported from two entirely different petrologic settings: (i) as a nanometer slab in a rutile twin bicrystal inclusion in garnet from diamondiferous quartzofeldspathic rocks from the Saxonian Erzgebirge (*15*), and (ii) in shocked gneisses from the Ries crater in Germany (*16*).

Recent diamond anvil cell (DAC) experiments on rutile up to total pressures in excess of 55 GPa established the existence of four dense polymorphs: (i) an orthorhombic α-PbO_2 phase (TiO_2 II, space group *Pbcn*), stable below 14 GPa at 300 K (*8*, *9*); (ii) a monoclinic baddeleyite-structured phase (M I, space group $P2_1/c$), stable above 14 GPa (*8*); (iii) an orthorhombic polymorph (O I, space group *Pbca*), stable above 28 GPa (*11*); and (iv) an orthorhombic cotunnite ($PbCl_2$)–structured polymorph (O II, space group *Pnma*), with nine-coordinated Ti, stable above 55 GPa (*10*).

The monoclinic baddeleyite-structured phase was never obtained in any shock-loading experiment. Instead, the α-PbO_2 phase was recovered from shock-loading experiments at pressure (P) > 20 GPa (*1*, *2*). This result was interpreted as suggestive of inversion of the baddeleyite-structured polymorph to the α-PbO_2 phase upon decompression (*1*, *2*).

It was inferred that rutile, in analogy to MnF_2, transforms by shock compression in the pressure range of 72 GPa to a distorted fluorite or fluorite-type structure (*12*, *13*). However, recent DAC experiments and ab initio calculations refute the existence of a distorted fluorite or fluorite-type structure in this pressure range (*10*, *16*, *17*).

The heavily shocked gneisses and amphibolites in the Ries suevite collected in the Altebürg, Otting, and Seelbronn localities belong to upper stage II of the progressive shock scale (*18–20*). The stabilities of both the ZrO_2-structured (M I, space group $P2_1/c$) polymorphs and the ZrO_2-related (O I, space group *Pbca*) polymorphs lie within this deformation stage (up to 30 GPa) (*16*). It appeared plausible that one or both polymorphs may be present and probably survived the post-shock temperature. A careful search for TiO_2 polymorphs denser than the α-PbO_2 phase in polished thin sections (PTSs) of the selected rock suite was conducted. Important criteria for the recognition of these phases are the expected higher reflectivity and different internal reflections in reflected light as a result of the higher densities (*14*). It is expected that the brightness of these polymorphs (M I and O I) in reflected light should be much higher than that of rutile, because these phases are 11.5 and 12.7% denser, respectively, than rutile.

We found a phase with optical reflectance remarkably higher than that of rutile in an assemblage of TiO_2 phases, ilmenite, and minor sphene. Electron microprobe analysis of rutile grains and the denser TiO_2 phase indicated that they are identical in composition: almost pure TiO_2, with minor concentrations of FeO and Nb_2O_5 (97.69% TiO_2, 0.14% FeO, and 0.20% Nb_2O_5). The new phase shows, in contrast to the white-to-yellow internal reflections of coexisting rutile, intense blue internal reflections in reflected polarized light and crossed polarizers (Figs. 1B and 2B). This is a characteristic diagnostic optical feature that serves to distinguish this phase from the α-PbO_2 polymorph, which has pink internal reflections (*16*). The new phase occurs in clusters of individual fine-grained polycrystalline monophase grains surrounded by large individual shock-twinned ilmenite grains and small rutile grains (Fig. 1) or as single grains surrounded by rutile, the α-PbO_2 phase, ilmenite, and sphene (Fig. 2). The new phase occupies the core of the assemblage, and the α-PbO_2 phase, ilmenite, and rutile occupy the outer regions (Fig. 2). We see no petrographic evidence of one TiO_2 polymorph replacing the other in the same grain.

We refrained from subjecting the assemblages to laser micro-Raman studies because of the instability of the ZrO_2-structured polymorphs (M I) and the denser orthorhombic (O I) polymorphs (*10*). The M I– and O I–TiO_2 phases synthesized in experiments above 14 and 28 GPa, respectively, are metastable and invert instantaneously upon laser irradiation at ambient pressure to the α-PbO_2–structured phase (*10*, *11*). We determined the structure of the new phase by x-ray microbeam diffraction techniques. A 0.8-mm disc containing the

[1]Max-Planck-Institut für Chemie, J. Joachim-Becher-Weg 27, 55128 Mainz, Germany. [2]Guangzhou Institute of Geochemistry, Chinese Academy of Science, Guangzhou, 510640, China. [3]Theoretical Geochemistry Program, Institute of Earth Sciences, Uppsala University, 75236 Uppsala, Sweden. [4]Laboratoire de Sciences de la Terre, Ecole Normale Supérieur de Lyon, 69364 Lyon, France.

*To whom correspondence should be addressed. E-mail: goresy@mpch-mainz.mpg.de

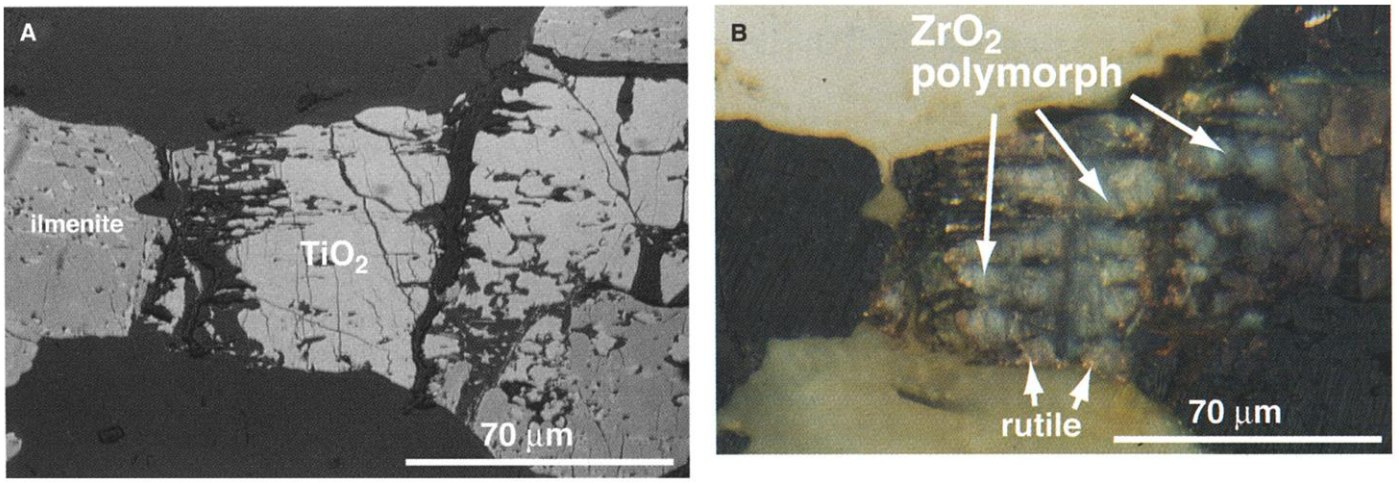

Fig. 1. A reflected light photograph displays a shocked opaque assemblage consisting of the new baddeleyite-structured polymorph of TiO_2, rutile, and ilmenite. (**A**) White in the central area and on the right side is the new phase and rutile; here indistinguishable from each other. Brown at the left and bottom right is ilmenite. The photograph was taken with plane-polarized light. (**B**) The same as in (A) with crossed polars. The material with blue internal reflections is the new monoclinic baddeleyite-structured (ZrO_2) TiO_2 polymorph. The very small grains at the lower edge of the new phase with white or yellow internal reflections (arrows) are rutile. The fussy appearance of the new phase is the result of the extremely fine-grained nature of the new mineral.

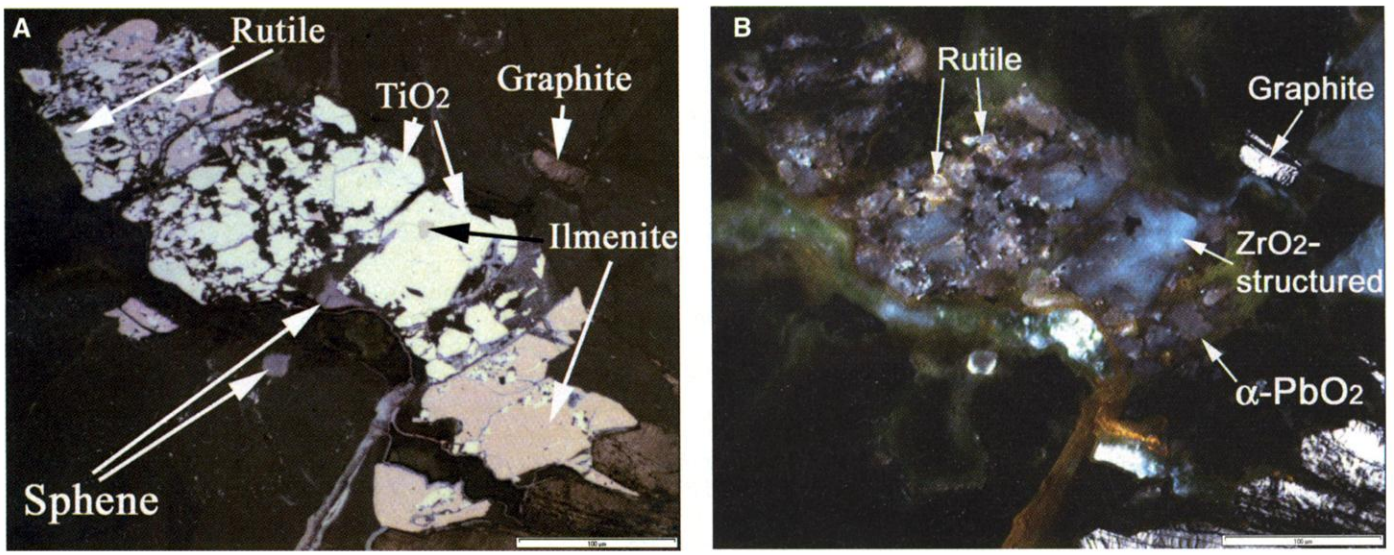

Fig. 2. (**A**) A reflected light photograph depicting a shocked opaque assemblage consisting of rutile, the α-PbO_2 polymorph, and the baddeleyite-structured polymorphs of TiO_2, along with ilmenite, sphene, and graphite. The photograph was taken with plane-polarized light. Length of the white bar on the bottom right is 100 μm. (**B**) The same as in (A) with crossed polars. The figure displays the textural relations and the internal reflections of the three TiO_2 polymorphs. The baddeleyite-structured polymorph (deep blue internal reflections) occupies the core of the opaque assemblage. Both less dense polymorphs, rutile (white internal reflections), and the α-PbO_2 phase (pink internal reflections) surround the new, very dense, baddeleyite-structured phase. Length of the white bar on the bottom right is 100 μm.

new phase and rutile (Fig. 1) was cored out from the PTS with a high-precision microdrill (*21*). We collected 21 x-ray reflections from the new phase in addition to the [110] reflection of rutile (Fig. 3 and Table 1). The new phase is sensitive to x-ray irradiation. The intensities of all x-ray reflections of this phase decreased progressively over the 18 hours of x-ray irradiation, and the intensity of the rutile reflection increased. Almost 50% of the new phase transformed within this time to rutile. The *d* spacings of all 21 x-ray reflections of the new phase (Fig. 3 and Table 1) are indexed in the framework of a monoclinic lattice with the following cell parameters: a = 4.606(2) Å, b = 4.986(3) Å, c = 4.933(3) Å, and β = 99.17(6)° (space group $P2_1/c$) (numbers in parentheses are standard deviations in the last significant digits). The positions of the diffraction lines and their relative intensities could be explained in terms of the baddeleyite (ZrO_2)–structured polymorph of TiO_2 (space group $P2_1/c$) (Fig. 3 and Table 1). The calculated density of the new phase is ρ = 4.72 g/cm^3. The baddeleyite ZrO_2–structured TiO_2 phase from the Ries crater is 11% denser than rutile. This is the first natural occurrence of an ultradense TiO_2 phase with Ti cations in seven-coordinated oxygen polyhedra.

We infer that the new phase formed by direct reconstructive phase transition from rutile. Formation by back-transformation through inversion of one of the denser orthorhombic O I polymorph, the $PbCl_2$-structured O II polymorph, or the cotunnite-structured O II polymorph would require much higher pressures [P = 28 to >60 GPa (*10*)]. Pressures at this range would have induced not only the inversion of quartz to stishovite but also melting in

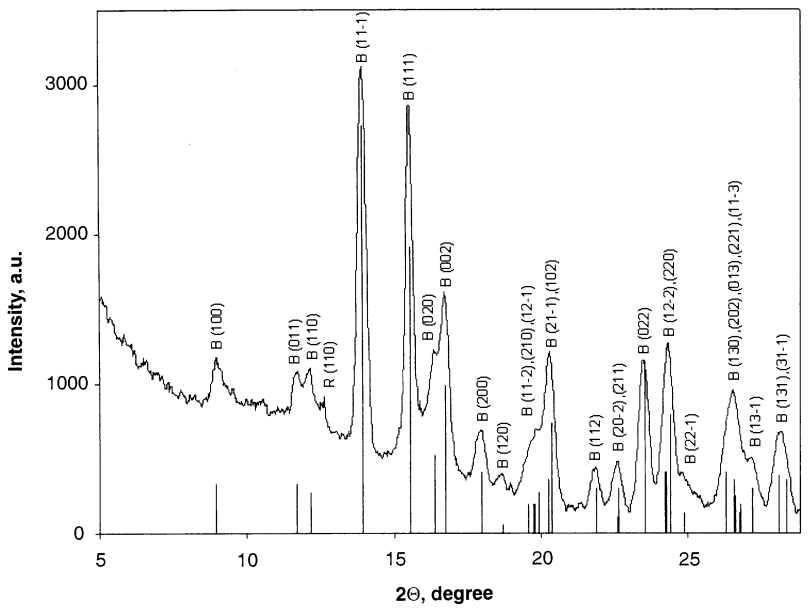

Fig. 3. X-ray diffraction pattern obtained from the central area of Fig. 1B. Twenty-one diffraction lines are indexed in the monoclinic baddeleyite structure (M I). One diffraction line (R 110) belongs to rutile (R) (Table 1).

feldspar and quartz in the shocked gneiss (*20*, *22*, *23*). We find no evidence of melting in feldspar or silica grains. Raman studies of the silica inclusions in garnet show that they are dense diaplectic glass with no evidence of coesite or stishovite (*18*, *20*, *22–24*). This entirely excludes the denser polymorphs as possible precursors. Consequently, the peak pressures very probably did not exceed 28 GPa. However, we cannot entirely exclude the possibility that the new phase formed by inversion of the O I phase.

The fabric setting of the monoclinic ZrO_2-structured phase is indicative that the original rutile grains in the core of the cluster experienced higher peak pressures than did the grains near the exterior and that pressure attenuated in the cluster outward during the impact event. Our x-ray diffraction analysis of the assemblage depicted in Fig. 1 revealed no evidence for the presence of the orthorhombic α-PbO_2–type phase (Fig. 3 and Table 1). This result supports the idea that the high-pressure polymorphs in the Ries event were preserved during the post-shock decompression period. This contradicts the results of static experiments (*8–11*). However, we may speculate that the presence of minor elements (0.14% FeO and 0.20% Nb_2O_5) could have been an important factor in preventing the expected back-transformation during decompression. Another possible reason for preservation of the new phase could be the existence of intrinsic post-shock stresses in the high-pressure assemblage in the oxide clusters. The following parameters of the Birch-Murnaghan equation of state were obtained for synthetic baddeleyite-type TiO_2 (*10*): KT = 304(6) GPa, K' = 3.9(2), and VO = 16.90(3) cm^3/mol. We obtained a molar volume of 16.82(2) cm^3/mol for the natural polymorph. This could indicate that the natural sample has a residual stress of about 1.5 GPa, which could stabilize the baddeleyite-type–structured TiO_2. Diaplectic SiO_2 glass in the same gneisses also shows evidence of residual stress. Raman spectra of diaplectic SiO_2 glass inclusions in garnet in the shocked gneisses are very similar to spectra collected from SiO_2 glass dynamically densified at 25 GPa (*22*, *23*, *28*).

The survival of the new polymorph of TiO_2 in the shocked gneisses of the Ries crater also provides additional evidence for very low post-shock temperatures. The post-shock temperature must have been far below the upper temperature bound of the orthorhombic α-PbO_2 phase (500°C).

A search for post-rutile polymorphs in the Tagamites of Popigai crater in Russia revealed no dense TiO_2 phases. This impactite was subjected to post-shock temperatures much in excess of 1000°C, thus leading to extensive melting (*29*) and back-transformation to polycrystalline rutile.

Rutile in subducted crust is expected to transform to the new phase in the lower regions of Earth's upper mantle or at the transition zone. Because this polymorph is isostructural with baddeleyite, it can accommodate appreciable amounts of ZrO_2 and HfO_2 in solid solution. This may change the fractionation and partitioning processes of these elements at the transition zone (660 km depth) and the lower mantle.

Table 1. Indexed peaks of the x-ray diffraction pattern and Miller indices collected from the natural baddeleyite-structured TiO_2 in the assemblage shown in Fig. 1, A and B.

d_{obs}* (Å)	I_{obs}† (%)	h	k	l	d_{calc}* (Å)	I_{calc}† (%)
4.548	11	1	0	0	4.547	12
3.486	12	0	1	1	3.484	12
3.357	14	1	1	0	3.359	11
3.247‡	3	1	1	0		
2.929	100	1	1	−1	2.931	100
2.626	91	1	1	1	2.625	70
2.494	24	0	2	0	2.493	19
2.437	42	0	0	2	2.435	37
2.276	14	2	0	0	2.273	15
2.188	3	1	2	0	2.186	2
2.07§	19	1	1	−2	2.092	7
		2	1	0	2.069	7
		1	2	−1	2.054	10
2.017	40	2	1	−1	2.017	40
		1	0	2		
1.873	10	1	1	2	1.870	11
1.814	3	2	0	−2	1.812	4
1.810	9	2	1	1	1.811	11
1.742	40	0	2	2	1.742	42
1.686	42	1	2	−2	1.693	15
		2	2	0	1.680	29
1.647	8	2	2	−1	1.649	6
1.54§	31	1	3	0	1.561	15
		2	0	2	1.544	13
		0	1	3	1.544	9
		2	2	1	1.533	5
		1	1	−3	1.534	7
1.510	12	1	3	−1	1.511	11
1.463	12	1	3	1	1.463	14
1.451	11	3	1	−1	1.452	13

*a = 4.606(2) Å, b = 4.986(3) Å, c = 4.933(3) Å, β = 99.17(6)°. †Intensities are calculated with lattice parameters given above and coordinates of atoms for the ZrO_2-structured TiO_2 polymorph. ‡Rutile reflection. §Broad reflections. d_{obs} and d_{calc} are observed and calculated d values, respectively. I_{obs} and I_{calc} are observed and calculated intensities, respectively.

References and Notes

1. R. G. McQueen, J. C. Jamieson, S. P. Marsh, *Science* **155**, 1401 (1967).
2. K. Linde, P. S. DeCarli, *J. Chem. Phys.* **50**, 319 (1969).
3. L. Liu, *Science* **199**, 422 (1978).
4. J. M. Léger, J. Haines, A. Atouf, P. Tomaszewski, *Am. Inst. Phys.* 363 (1994).
5. J. Haines, J. M. Léger, *Phys. Rev. B* **55**, 1 (1997).
6. _____, O. Schulte, *Science* **271**, 629 (1996).
7. _____, *J. Phys. Condens. Matt.* **8**, 1631 (1996).
8. L. Gerward, J. S. Olsen, *J. Appl. Crystallogr.* **30**, 259 (1997).
9. J. S. Olsen, L. Gerward, J. Z. Jiang, *J. Phys. Chem. Solids* **60**, 229 (1999).
10. L. S. Dubrovinsky *et al.*, *Nature* **6829**, 653 (2001).
11. N. A. Dubrovinskaia, L. S. Dubrovinsky, V. B. Prokopenko, R. Ahuja, V. Dmitrev, in preparation.
12. Y. Syono, K. Kusaba, M. Kikushi, K. Fukuoka, T. Goto, *Shock-Induced Phase Transitions in Rutile Single Crystal*, M. H. Manghani, Y. Syano Eds. (Terra/American Geophysical Union, Washington, DC, 1987).
13. K. Kusaba, M. Kikuchi, K. Fukuoka, Y. Syono, *Phys. Chem. Miner.* **15**, 238 (1988).
14. P. Ramdohr, *Die Erzmineralien und ihre Verwachsungen* (Akademie-Verlag, Berlin, Germany, ed. 4, 1975).
15. S.-L. Hwang, P. Shen, H.-T. Chu, T.-F. Yui, *Science* **288**, 321 (2000).
16. A. El Goresy, M. Chen, P. Gillet, L. S. Dubrovinsky, G. Graup, *Earth Planet. Sci. Lett.*, in press.
17. R. Ahuja, unpublished data (2001).

18. D. Stöffler, *Fortschr. Mineral.* **49**, 50 (1972).
19. _____, *Fortschr. Mineral.* **51**, 256 (1974).
20. A. El Goresy *et al.*, *Am. Mineral.* **86**, 611 (2001).
21. The x-ray facility used in this study includes a rotating anode generator (18 kW), a capillary collimating system, and a charge-coupled device (CCD) area detector. The radiation from the rotating anode with a molybdenum target is filtered by a zirconium foil so that the intensity of Kβ x-ray reflection is 1% of that of Kα x-ray reflection. The beam of initial size 1 mm by 0.5 mm is collimated to 0.1-mm diameter using the capillary system. A special collimator was used to reduce the size of the x-ray spot to 40 μm full width at half maximum. The diffracted x-rays were collected on a detector with an area of 512 by 512 pixels. Data were acquired at fixed 2θ settings of 15, 25, and 30 and a sample-to-detector distance of 210 mm. Collection time in different points varied from 15 min to 12 hours. Settings of the detector were calibrated with external independent standards (W, MgO, and Al_2O_3) at each position of the detector. The sample disc was mounted on a 0.8-mm hole in a large steel disc that was loaded onto the goniometer stage. We rotated the sample plate 30° from the initial position normal to the x-ray beam with a step of 1° in the ω axis during data collection. The position of the collimated x-ray beam penetrating through the rutile-ZrO_2–structured polymorph-bearing assemblage was continuously monitored on a screen with a CCD camera.
22. V. Stähle, P. Gillet, M. Chen, A. El Goresy, *Meteorit. Planet. Sci.* (1999).
23. _____, unpublished data.
24. E. C. T. Chao, *Science* **156**, 192 (1967).
25. P. S. DeCarli, A. P. Jones, G. D. Price, *Laboratory Impact Experiments and Calculations vs. Natural Impact Events. Catastrophic Events & Mass Extinctions: Impacts and Beyond* (Lunar and Planetary Institute, Vienna, 2000).
26. P. S. DeCarli, E. Bowden, T. G. Sharp, A. P. Jones, G. D. Price, *Lunar Planet Sci.* **XXXII**, abstract 3090 (2001).
27. A. El Goresy, L. S. Dubrovinsky, T. G. Sharp, S. K. Saxena, M. Chen, *Science* **288**, 1632 (2000).
28. M. Okuno, B. Reynard, Y. Shimada, Y. Syono, C. Williame, *Phys. Chem. Mineral.* **26**, 304 (1999).
29. V. L. Masaitis, *Meteorit. Planet. Sci.* **33**, 349 (1998).
30. M.C. was supported by the National Science Foundation of China (grant 49825132) and Deutsche Forschungsgemeinschaft (Go 315/15-1). The manuscript benefited from constructive reviews by two anonymous reviewers. We are indebted to O. Medenbach of Ruhr Universität Bochum for his aid in precisely coring out the assemblage depicted in Fig. 1 for microbeam x-ray diffraction.

8 May 2001; accepted 11 July 2001

Large Groundwater Strontium Flux to the Oceans from the Bengal Basin and the Marine Strontium Isotope Record

Asish R. Basu,[1]* Stein B. Jacobsen,[2] Robert J. Poreda,[1] Carolyn B. Dowling,[1] Pradeep K. Aggarwal[3]

Strontium concentration and isotopic data for subsurface flowing groundwaters of the Ganges-Brahmaputra (G-B) delta in the Bengal Basin demonstrate that this is a potentially significant source of strontium to the oceans, equal in magnitude to the dissolved strontium concentration carried to the oceans by the G-B river waters. The strontium concentrations of groundwaters are higher by a factor of about 10 than typical G-B river waters and they have similar $^{87}Sr/^{86}Sr$ ratio to the river waters. These new data suggest that the present contribution of the G-B system to the rise in $^{87}Sr/^{86}Sr$ ratio in seawater is higher by at least a factor of 2 to 5 than the average over the past 40 million years.

Variations of $^{87}Sr/^{86}Sr$ ratio in seawater are primarily due to variations in continental erosion rates as well as variations in the Sr isotopic composition of this input to the oceans (*1, 2*). Thus, changes in this isotopic ratio are frequently linked to major tectonic events (*3, 4*) and have been used to constrain the problem of Snowball Earth glaciations (*5*). The $^{87}Sr/^{86}Sr$ ratio of seawater has increased from about 0.7078 to 0.7092 over the past 40 million years (My). This rapid increase has been attributed to the Himalayan uplift, following the India-Asia continental collision (*2*), which is believed to have contributed Sr with particularly high $^{87}Sr/^{86}Sr$ ratios to the oceans through the major rivers draining the Himalayas (*3, 4, 6, 7*). The Himalayan uplift has also been suggested as the major cause of the global climate cooling for the past 40 My, because of the increase in chemical weathering of silicates and the resulting decrease of atmospheric CO_2 concentration (*8*).

Most workers accept the importance of the contribution of Himalayan river water dissolved Sr for the marine budget, although the sources and the amount of this Sr flux remain problematic (*9*). Various calculations based on Sr isotopic compositions and Sr concentrations of the G-B rivers indicate that the Himalayan discharge accounts for a large fraction of the observed increase in the marine $^{87}Sr/^{86}Sr$ ratio over the past 40 My (*4, 6*). However, a study of Himalayan riverine $^{187}Os/^{188}Os$ (*10*) could not explain the observed correlated Sr-Os isotopic shift in the marine record by Himalayan input. There is also uncertainty whether the Sr flux and its isotopic composition are primarily controlled by the weathering of silicate minerals (*6, 9, 11, 12*) or are controlled by weathering of metacarbonates that reequilibrated with silicates with high $^{87}Sr/^{86}Sr$ during metamorphism (*7, 13, 14*), or both.

Most earlier studies focused on the weathering of high Himalayan rocks. Here, we are concerned with the effect of groundwater-sediment interaction processes in the G-B flood plain of the Bengal Basin (Fig. 1) in controlling the budget of oceanic Sr as well as the Sr isotopic composition of seawater. This study was prompted by the recent discovery of large groundwater flux on a regional scale to coastal waters (*15*) and that desorption of ^{226}Ra and Ba from deltaic sediments in this area is a significant source of these elements in the waters of the Bay of Bengal (*16*). There is clear evidence of a large groundwater discharge with high Ra and Ba fluxes to the ocean from the G-B rivers during low river discharge (*17*).

For this study, we collected 61 groundwater samples from the southern part of Bangladesh between the Ganges (Padma), Brahmaputra, and Meghna rivers and their tributaries, and nine groundwater samples just north and south of Calcutta in the western part of the basin (Fig. 1). The water samples come from depths of 10 to 350 m. We also collected river waters from six sites of the G-B system within and adjacent to the Bengal Basin (Fig. 1 and Table 1). All the river and groundwater samples were collected during the dry season in January through May and were filtered (0.2 μm pore size) and acidified on site. The Sr concentration and $^{87}Sr/^{86}Sr$ ratios are reported in Table 1. For individual sites where more than one groundwater sample was analyzed from different depths, Table 1 gives the range and average values for Sr. For many of the groundwater samples, we also examined other chemical characteristics, such as dissolved cations and anions, carbon, oxygen, and hydrogen isotopes for all samples, and ^{3}H-^{3}He ages for several of the samples. Here, we are concerned mostly with the $^{87}Sr/^{86}Sr$ and Sr concentrations in these waters, and implications of a groundwater Sr flux on the marine Sr budget.

The Sr concentrations in the groundwater

[1]Department of Earth and Environmental Sciences, University of Rochester, Rochester, NY 14627, USA. [2]Department of Earth and Planetary Sciences, Harvard University, Cambridge, MA 01238, USA. [3]Isotope Hydrology Section, International Atomic Energy Agency, Post Office Box 100, A1400, Vienna, Austria.

*To whom correspondence should be addressed. E-mail: abasu@earth.rochester.edu